

Seismic Performance Evaluation of Steel Moment Resisting Frames Designed Using the Performance-Based Plastic Design Approach

T.Y. Yang, M. Baradaran Shoraka & J. Jiang

University of British Columbia, Vancouver, Canada

M.R. Bayat

Englekirk Structural Engineers, California, USA

S.C. Goel

University of Michigan, Ann Arbor, USA



SUMMARY:

Conventional design of seismic force resisting systems typically follows the equivalent static force procedure (ESFP), where the elastic seismic design force is reduced by a reduction factor to account for the structure's ability to deform inelastically, i.e., ductility capacity. This is achieved by designing the elements and connections in a ductile manner. The system is then checked to ensure the inelastic deformations do not exceed the ductility capacity in the connections and elements. The performance-based plastic design (PBPD) approach, on the other hand, pre-selects a plastic mechanism to satisfy both the inelastic drift and strength limits in the initial design. This design approach eliminates the need to pre-select a reduction factor and iteratively design the structure to meet the prescribed deformation limit. To assess the seismic performance of the systems designed using such approach, a prototype building located in Los Angeles, California was designed using both the conventional code-based ESFP and the proposed PBPD approaches. Detailed nonlinear analytical models for each of the designs were developed. A site specific seismic hazard analysis was conducted and sets of ground motions representing multiple hazard levels were applied to the models to simulate the nonlinear dynamic response of the systems. Both the structural responses, the structural material usage and the lifetime maintenance cost are systematically compared and presented in this paper.

Keywords: Performance-based plastic design; Steel moment frame; Earthquake Engineering; Seismic loss

1. INTRODUCTION

Conventional design of seismic force resisting systems typically follows the equivalent static force procedure (ESFP), where the elastic seismic design force is reduced by a reduction factor to account for the structure's ability to deform inelastically. This is achieved by designing the elements and connections in a ductile manner. The system is then checked to ensure the inelastic deformations do not exceed the ductility capacity in the connections and elements. This design approach does not account for the nonlinear response of the entire system which might lead to severe yielding and buckling of structural members. In some severe cases, this might lead to total collapse or extensive repair costs. In order to achieve more predictable system performance under strong earthquake ground shaking, knowledge of the ultimate structural behaviour, such as the nonlinear relations between force and deformation, and yield mechanism of the structure are essential. One such complete design methodology has been developed by Goel and Chao (2008). The method is called the Performance-Based Plastic Design (PBPD) method. The PBPD method uses pre-selected target drift and yielding mechanism to design the structural system to meet both the drift and strength limits using the plastic design approach. This approach practically eliminates the need for additional iteration after initial design.

Despite the apparent advantages of the PBPD approach, the relative seismic performance of the system designed using the PBPD approach throughout its life cycle cost has not been demonstrated. To compare the seismic performance of the systems designed using the conventional code-based (ESFP) methods and the PBPD approaches, a twenty-story office building located in Los Angeles, California was studied in this paper. The code-based design was originally designed as part of the

SAC Steel Research Program (Gupta and Krawinkler 1999). The prototype building was also designed using the PBPD approach (Goel and Chao 2008; Bayat 2010). A detailed performance assessment of the prototype building using each of these two design approaches was carried out using the performance-based assessment methodology presented by Yang et al. (2009a). This methodology used a Monte-Carlo simulation procedure in which the building was analyzed under numerous earthquake ground motions, with repair costs aggregated to determine rates at which different repair costs occur. To carry out the procedure, major structural and non-structural components of the building were identified and grouped into performance groups. Damage fragility relations, corresponding repair methods, repair material quantities and repair cost functions were defined for each performance group. Finite element models of the buildings, one for each of the design approaches were developed. Nonlinear dynamic analyses for individual earthquake ground motion records were conducted to establish peak response quantities. Detailed statistical distribution was fitted to the peak response quantities and used with the fragility functions to determine the damage state of each performance group. Once the damage states had been identified, the repair cost was then calculated based on the repair action in each of the damage states. The repair cost of the building was then calculated by summing the repair cost of each performance group. The process was repeated a large number of times to simulate the distribution of the repair costs. The results of the performance assessment were then used to compare the relative performance merits of the prototype building designed using the code-based and the PBPD approaches.

2. DESCRIPTION OF THE PROTOTYPE BUILDINGS

A prototype of a twenty-story (five bays by six bays) office building without basement level was selected for this study. Two designs of this prototype were compared. The first design was originally designed as part of the SAC Steel Research Program (Gupta and Krawinkler 1999) and the second design was re-designed by the PBPD approach (Goel and Chao 2008; Bayat 2010). The prototype had a fixed bay width of 6.1 m (20 feet), a first-floor height of 5.5 m (18 feet), and a floor height of 4 m (13 feet) at other floors. The building plan and elevation of the N-S perimeter moment frame are shown in Fig. 2.1 and Fig. 2.2, respectively. Since the original SAC frame was designed based on the 1994 Uniform Building Code (UBC 1994), for comparison purposes the same loading and design criteria were used for the redesign of the PBPD building. The material weights for the seismic force resisting system are compared in Table 2.1. Overall, the code-based design used approximately 7% more structural steel in the beams but 20% less in the columns. This results in a total of 13% more structural steel in the PBPD design as compared to the code-based design. It should be noted that such ratio will be less significant if the total weight (including the gravity system) of the building is included in the comparison.

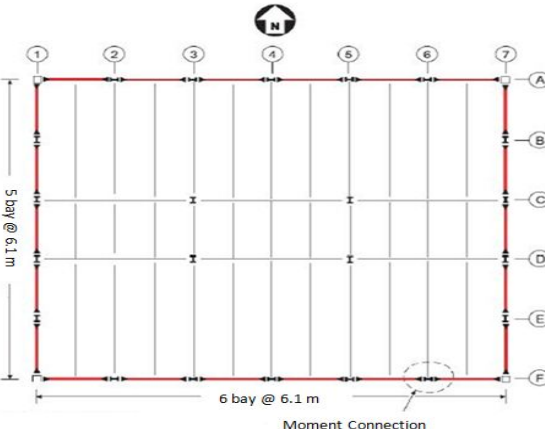


Figure 2.1. Plan view of the prototype model

Table 2.1. Material Weight for One Moment Frame (5 Bays)

Weight	PBPD (kN)	Code-based Design (kN)
Beams	794	853
Columns	1770	1419
Total	2564	2272

3. PERFORMANCE GROUPS AND DAMAGE STATES

Major components of the prototype building were assigned to 101 performance groups (PGs). These include: one structural PG at each floor level (1-20), one exterior (21-40) and one interior (41-60) drift-sensitive non-structural component PG at each floor, one interior acceleration-sensitive non-structural component PG at each floor (61-80), one acceleration-sensitive content PG at each floor (81-100) and one HVAC PG at the roof (101). The PGs were selected based on a collection of components whose performance was similarly affected by a particular engineering demand parameter (EDP). For example, the structural components were assigned to PGs whose performance was associated with inter-story drift in the story where the components were located. The non-structural components were divided into displacement and acceleration groups. The displacement groups used inter-story drift ratios to define the performance, while the acceleration groups used total floor accelerations. Multiple damage states were defined for each PG. These states correspond to different levels of damage and the repair actions. For example, the drift-sensitive structural component performance group at the second floor (PG 2) has four states. States range from none (DS1) to minor (DS2) to severe damage (DS3) and finally collapse (DS4). For each state, a model (fragility relation) defines the probability of damage being less than or equal to the threshold damage, given the value of the EDP associated with the PG. Fig. 3.1. shows the fragility curves defined for PG 2. In this figure, if the inter-story drift ratio is 2.0%, the PG has a 12.5% probability in DS1, 64.7% probability in DS2, 19.7% probability in DS3 and 3.1% probability in DS4. Table 3.1. shows a summary of the performance groups included in this study. Symbols $\delta_{i,j}$ and a_i represent the inter-story drift ratio at the i th story and the total floor acceleration at the i th floor, respectively. The performance groups presented in this study are obtained from the ATC 58 research team (Applied Technology Council 58, 2008) and the values used in this study are summarized in Yang et al. (2009b).

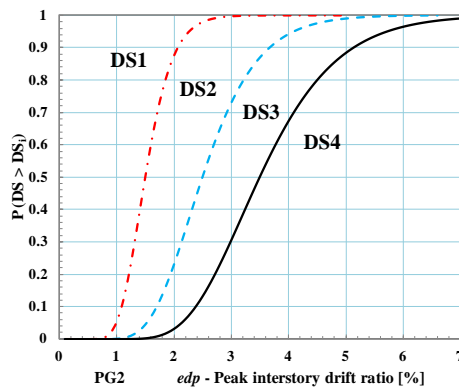


Figure 3.1. Example of fragility curves (Yang et al. 2009a)

Table 3.1. Summary of performance groups

Performance Group	Name	Location	Engineering Demand Parameters
01-20	CL12-CL20R	between levels 1 & 2 - between levels 20 & Roof	du1 – du20
21-40	EXTD12-EXTD20R	between levels 1 & 2 - between levels 20 & Roof	du1 – du20
41-60	INTD12-INTD20R	between levels 1 & 2 - between levels 20 & Roof	du1 – du20
61-80	INTA2-INTAR	below levels 2 – below level Roof	a2 – aR
81-101	CONT1-CONTR	level 1 - level Roof	a1 – aR

4. STRUCTURAL MODELS

Analytical models of the building were created for the two designs. The models were developed using Perform-3D (CSI, 2007). For simplicity, only the response in the North-South direction is presented in this paper.

A uniform modeling procedure was established for both models to allow the engineering demand parameters (EDPs) to be compared. 2D nonlinear finite element models were built using Perform-3D (CSI, 2007). The beams and columns were modeled with elastic elements with lumped plastic hinges and rigid end zones at each end. The nonlinear hinges were defined using tri-linear backbone curve, where the ultimate moment capacity (Mp) was estimated using the expected material properties and nominal strain hardening. Moment capacity degrades linearly to 0.1Mp for plastic rotations between 0.04 radian and 0.1 radian. Cyclic degradation was not modeled in the plastic hinges. Panel zones were modeled using the approach presented by Krawinkler (1978). For column elements, an additional moment-axial force interaction curve was used to calculate structural response. The gravity columns were modeled using a “P-delta column”. Seismic masses were lumped at the nodes according to the tributary area. Rayleigh damping of 2% was assigned to the 1st and 3rd mode in the building models. Table 4.1. shows the first five modal periods of the two designs.

Table 4.1. Periods for the two design approaches

Mode	Code Design [seconds]	Performance-Based Plastic Design [seconds]
T1	3.9	3.8
T2	1.4	1.4
T3	0.8	0.8
T4	0.6	0.5
T5	0.4	0.4

5. GROUND MOTION SELECTION

A detailed seismic hazard analysis was conducted for the building. Five hazard levels representing the 1% probability of exceedance in 50 years (1/50), 2% probability of exceedance in 50 years (2/50), 5% probability of exceedance in 50 years (5/50), 10% probability of exceedance in 50 years (10/50) and 20% probability of exceedance in 50 years (20/50) are included in this study. A total of 20 ground motions were selected for each of the hazard levels. Ground motions were taken from the PEER NGA database (PEER, 2011) with the target spectrum suggested by the SAC Steel Research Program (Somerville et al., 1997). The ground motions were amplitude scaled such that the mean spectrum of the set of ground motions over the period range from $0.2T_1$ to $1.5T_1$ (with T_1 being the first vibrational period of the structure) did not fall below the target spectrum by 10%. Since the first vibrational period was very similar between both designs, a first modal period of 3.8 sec was used to scale the ground

motions for both. Fig. 5.1. shows an illustrative example of the scaled spectra for the 1/50 hazard level. Tables 5.1. to 5.5. list the selected ground motions used in this study.

Table 5.1. Selected records 20% in 50 years hazard

Event	Year	R (km)	Magnitude Mw
Northridge	1994	17	6.7
Landers	1992	27	6
Big Bear	1992	10.2	6.5
Big Bear	1992	38.3	6.5
Morgan Hill	1984	20	6
Imperial Valley	1979	4.1	6.5
Imperial Valley	1979	6.2	6.5
Parkfield	1966	19.3	6.5
Parkfield	1966	16	6.5
Imperial Valley	1940	10	6.9

Table 5.2. Selected records 10% in 50 years hazard

Event	Year	R (km)	Magnitude Mw
Northridge	1994	6.7	6.7
Northridge	1994	7.5	6.7
Northridge	1994	6.4	6.7
Landers	1992	36	7.3
Landers	1992	25	7.3
Loma Prieta	1989	12.4	7
N. Palm Springs	1986	6.7	6
Imperial Valley	1979	4.1	6.5
Imperial Valley	1979	1.2	6.5
Imperial Valley	1940	10	6.9

Table 5.3. Selected records 5% in 50 years hazard

Event	Year	R (km)	Magnitude Mw
Kobe	1995	6.7	6.9
Northridge	1994	7.5	6.7
Northridge	1994	5	6.7
Big Bear	1992	10	6.5
Loma Prieta	1989	12.4	7
Superstition Hills	1987	11	6.5
Superstition Hills	1987	16	6.5
Imperial Valley	1979	6.2	6.5
Imperial Valley	1979	4.1	6.5
Imperial Valley	1940	10	6.9

Table 5.4. Selected records 2% in 50 years hazard

Event	Year	R (km)	Magnitude Mw
Elysian Park	(simulated)	1.5	7.1
Elysian Park	(simulated)	1.5	7.1
Elysian Park	(simulated)	11.2	7.1
Elysian Park	(simulated)	10.7	7.1
Elysian Park	(simulated)	17.5	7.1
Kobe	1995	3.4	6.9
Northridge	1994	7.5	6.7
Northridge	1994	6.4	6.7
Loma, Prieta	1989	3.5	7
Tabas	1974	1.2	7.4

Table 5.5. Selected records 1% in 50 years hazard

Event	Year	R (km)	Magnitude Mw
Kocaeli - Turkey	1999	15.4	7.5
Northridge	1994	26.4	6.7
Northridge	1994	23.4	6.7
Northridge	1994	6.5	6.7
Loma Prieta	1989	24.8	6.9
Imperial Valley	1979	22	6.5
Imperial Valley	1979	7	6.5
Imperial Valley	1979	5.1	6.5
Imperial Valley	1979	3.9	6.5

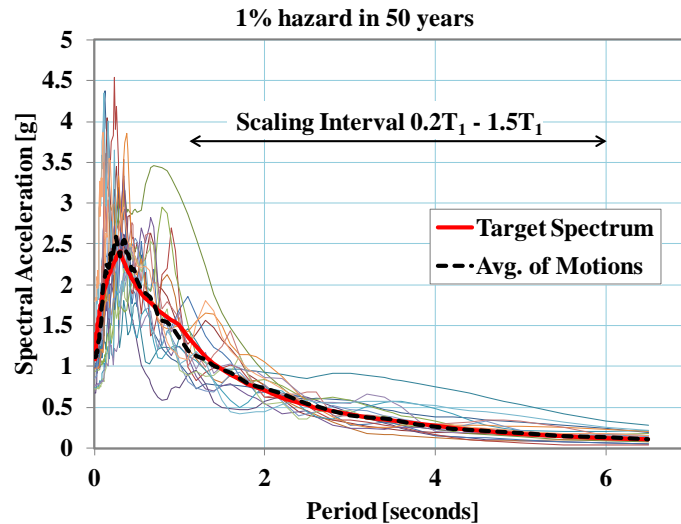


Figure 5.1 Example of ground motion scaling procedure for 1% in 50 years hazard

6. SEISMIC RESPONSE QUANTIFICATION

Nonlinear dynamic analyses were conducted to determine the seismic response of the two designs to each of the scaled ground motions. Using the approach presented in FEMAP695 (2009), the structure was considered to have collapsed when the maximum inter-story drift ratio exceeded 10%. In this study, the results indicate that both systems behaved as intended, where no collapse was observed at the lower intensity hazard levels (20/50, 10/50 and 5/50). As the hazard increased to 2/50, 3 out of the 20 ground motions caused collapse (excessive drift limit) in the code-based design, while collapse was not observed in the PBPD design. At the 1/50 hazard level, for the code-based design, 5 out of 20 ground motions experienced collapse while for the PBPD design only 3 out of 20 ground motions experienced collapse. Table 6.1. summarizes the number of collapse cases at each hazard level.

By separating the results for ground motions which did not cause collapse, Table 6.1. shows the median peak inter-story drift and total floor acceleration recorded from the time history analyses. Table 6.2. shows the corresponding standard deviation of the peak inter-story drift and total floor acceleration recorded from the time history analyses. The result shows, in general, the code-based designed building has slightly higher median story drift and higher dispersion (higher standard deviation) as compared to the PBPD structure. The difference becomes more significant as the earthquake shaking intensities increase. On the other hand, the median peak floor accelerations are very comparable between both designs for all the hazard levels considered.

7. COMPUTE THE REPAIR COSTS

The computed response results presented in Tables 6.2. and 6.3. were used in a mathematical model to systematically generate a large number of additional simulated response maxima having the same statistical properties as the original set. Detailed procedure to synthetically generate the large array of EDP matrix was presented in Yang et al. (2009a). The generated EDP matrix was then used to identify the damage states of each performance groups. Once the damage state of each performance group was identified, the repair action and associate repair cost for each performance group shown in Table 3.1. was then calculated. Finally, the total repair cost for the entire building was then summed over all performance groups. The process was repeated a large number of times to quantify the distribution of the repair costs at different levels of earthquake shaking intensity. The results of the non-collapse cases were then combined with the collapse cases using the performance-assessment procedure as presented in Baradaran Shoraka et al. (2012). Fig. 7.1.a and 7.1.b show the lognormal cumulative distribution functions of the total repair costs normalized with respect to the total replacement cost for

the low and high shaking intensities, respectively. The results showed that at the lowest shaking intensity (20/50), the PBPD and code-based design had roughly identical loss distribution. As the shaking intensity increased to 10/50 and 5/50 hazard levels, the code-based design resulted in higher loss than the PBPD structure. As the shaking intensity increased to 2/50 and 1/50 hazard levels, the results (Fig. 7.1.b) clearly indicate that the PBPD design was more robust than the code-based design. The jump in the repair cost at the 2/50 and 1/50 hazard levels was contributed from the scenario of the collapse cases. At the 1/50 hazard level the collapse scenario contributes about 25% of the total repair cost distribution for the code-based design.

The results of the performance assessment can also be presented using the annualized loss as described in Yang et al. (2009a). Fig. 7.2. shows the annualized repair cost for the two designs. As shown in this figure, the PBPD approach resulted in lower annualized repair cost as compared to the code-based design. In addition, the area under the annualized loss curve represents the mean annualized loss. The result showed that the mean annualized loss was about 0.67% and 0.71% of the total replacement value of the building for the PBPD and code-based approach, respectively. If the total replacement value of the building was \$50 million, then this would result in \$20,000 reduction in annualized repair cost with the PDPB design as compared with the code-based design.

Table 6.1. Number of collapse cases for each hazard level for the two design approaches

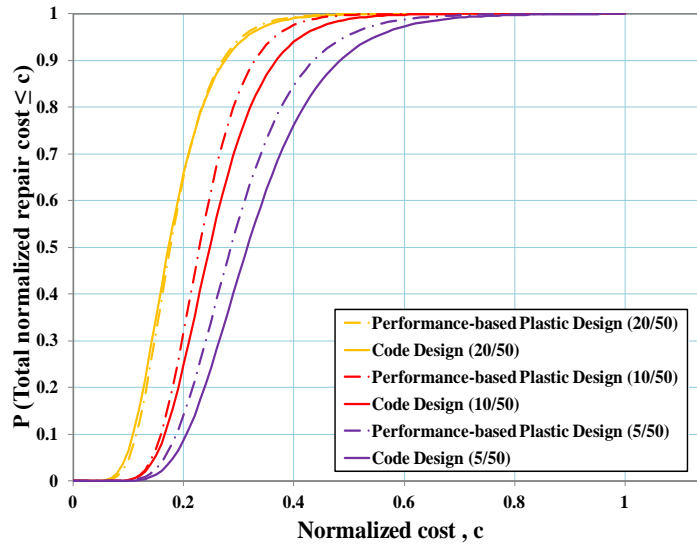
Building	20/50	10/50	5/50	2/50	1/50
Code	0 out of 20	0 out of 20	0 out of 20	3 out of 20	5 out of 20
PBPD	0 out of 20	3 out of 20			

Table 6.2. Median peak inter-story drift ratio and floor acceleration

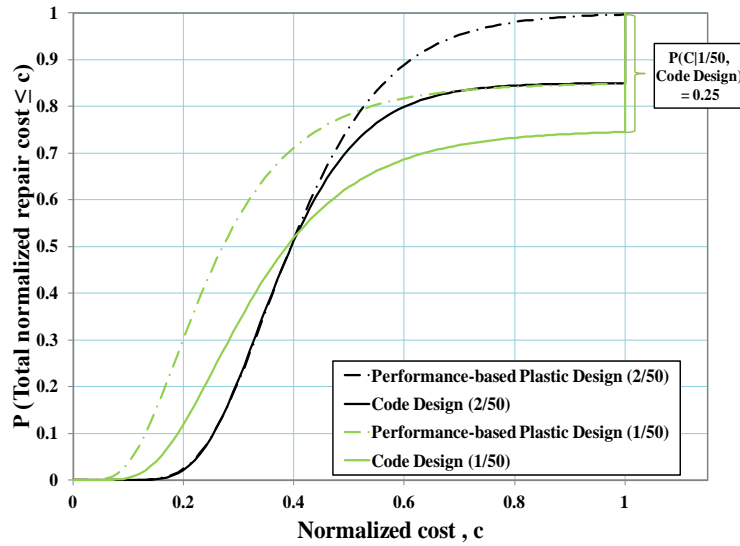
Hazard	Building	du2 [%]	du3 [%]	du4 [%]	du5 [%]	duR [%]	ag [g]	a2 [g]	a3 [g]	a4 [g]	a5 [g]	aR [g]
20/50	Code	0.7	0.6	0.6	0.6	0.9	0.6	0.4	0.4	0.4	0.4	0.6
	PBPD	0.6	0.6	0.6	0.6	1.1	0.6	0.5	0.4	0.4	0.4	0.6
10/50	Code	1.1	1.2	1.1	1.2	1.3	0.6	0.5	0.4	0.4	0.4	0.6
	PBPD	1.0	1.1	1.1	1.2	1.5	0.6	0.5	0.5	0.5	0.5	0.7
5/50	Code	1.0	1.1	1.1	1.1	1.4	0.7	0.6	0.6	0.6	0.5	0.7
	PBPD	0.9	1.0	1.0	1.1	1.7	0.8	0.6	0.6	0.5	0.5	0.8
2/50	Code	1.9	1.9	1.8	1.8	1.9	0.8	0.7	0.7	0.7	0.7	0.7
	PBPD	1.5	1.7	1.8	1.9	2.1	0.9	0.7	0.7	0.7	0.7	0.8
1/50	Code	1.8	1.8	2.0	1.9	1.8	1.1	0.8	0.8	0.8	0.8	0.7
	PBPD	1.5	1.6	1.8	2.0	2.4	1.2	0.8	0.8	0.8	0.8	0.9

Table 6.3. Standard deviation of peak inter-story drifts ratio and floor acceleration

Hazard	Building	du2 [%]	du3 [%]	du4 [%]	du5 [%]	duR [%]	ag [g]	a2 [g]	a3 [g]	a4 [g]	a5 [g]	aR [g]
20/50	Code	0.3	0.3	0.3	0.3	0.3	0.4	0.2	0.1	0.1	0.1	0.1
	PBPD	0.2	0.3	0.3	0.3	0.4	0.4	0.2	0.2	0.1	0.1	0.2
10/50	Code	0.3	0.4	0.5	0.6	0.3	0.2	0.1	0.1	0.1	0.1	0.1
	PBPD	0.2	0.3	0.5	0.6	0.4	0.2	0.1	0.1	0.1	0.2	0.2
5/50	Code	0.3	0.3	0.3	0.3	0.3	0.3	0.2	0.2	0.2	0.2	0.1
	PBPD	0.2	0.3	0.3	0.3	0.4	0.3	0.2	0.2	0.2	0.2	0.1
2/50	Code	1.0	1.0	0.9	0.9	0.4	0.3	0.3	0.2	0.2	0.2	0.1
	PBPD	3.1	2.7	2.4	2.1	0.6	0.3	0.2	0.2	0.2	0.2	0.1
1/50	Code	1.9	1.8	1.6	1.2	0.3	0.7	0.4	0.3	0.3	0.2	0.1
	PBPD	1.0	1.1	1.1	1.1	0.5	0.6	0.4	0.3	0.3	0.2	0.1



(a) Low – moderate hazard levels



(b) High hazard levels

Figure 7.1. Cumulative Distribution Functions for normalized cost at 5 different hazard levels considering different collapse criteria, [normalized cost = repair cost / (replacement cost)]

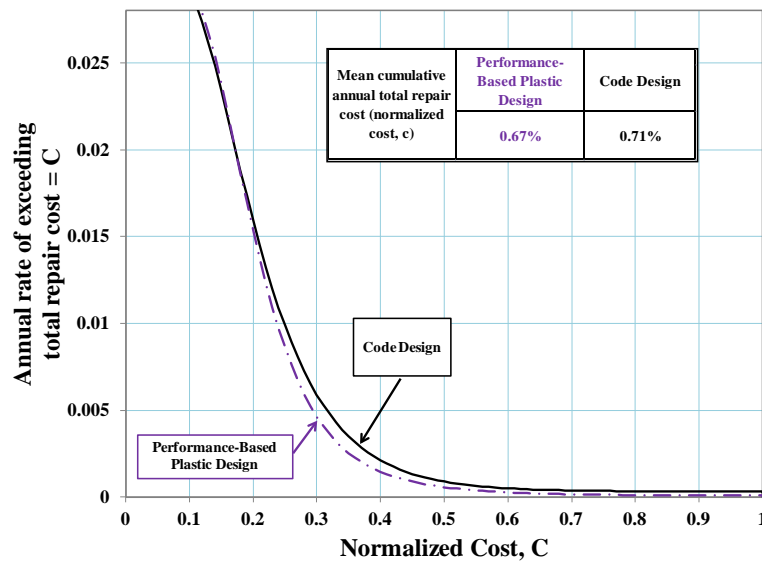


Figure 7.2. Annualized total repair cost

8. SUMMARY AND CONCLUSIONS

An alternative design approach, the Performance-Based Plastic Design (PBPD) method, had been developed by Goel and Chao (2008). This method used the energy-based approach to design the structural system by directly accounting for the plastic mechanism of the system. Designated yielding members were selected to dissipate the earthquake energy, while the remaining structures were capacity designed to remain linearly elastic. Such design approach eliminated the need to conduct iterative designs for the structural system to meet the strength and deformation limits. The seismic performance of the PBPD design approach is studied in this paper. A prototype 20 story steel moment resisting frame office building designed using the conventional code-based approach and PBPD approach was used as the basis for the comparison. Detailed finite element models were developed for each of the design approaches. Nonlinear dynamic responses of the structures under five levels of earthquake intensities were analyzed. The results showed the PBPD frame was more robust than the code-based design, where it had less probability of collapse at higher earthquake shaking intensities. State-of-the-art loss simulation analysis was completed using the procedure presented in Yang et al. (2009a). The results showed the PBPD design had less structural repair cost as compared to the code-based design approach for all hazard levels considered. The results provided the needed information to demonstrate the robustness of the PBPD design.

ACKNOWLEDGEMENTS

This work was funded in part by the Natural Sciences and Engineering Research Council of Canada (NSERC) jointly with the Steel Structures Education Foundation (SSEF). The authors would like to acknowledge Dr. S. Leelataviwat, Dr. D.C. Rai, Dr. W.C. Liao, Dr. S.H. Chao and Dr. B. Stojadinovic for providing valuable input to this project. Members of the ATC-58 project team for providing fragility curves, repair method and repair cost information for the performance groups used in this study. Any opinions, findings and conclusion or recommendations expressed in this material are those of the authors and do not necessarily reflect those of the Natural Sciences and Engineering Research Council of Canada or the Steel Structures Education Foundation.

REFERENCES

- Applied Technology Council 58, 2008. Development of next-generation performance-based seismic design procedures for new and existing buildings. Applied Technology Council, <http://www.atccouncil.org/atc-58.shtml>.
- Baradaran Shoraka, M., Yang, T. Y., and Elwood, K. J. (2012). Seismic loss estimation of non-ductile reinforced concrete buildings. *Earthquake Engineering and Structural Dynamics*, Manuscript accepted for publication.
- Bayat, M. R. (2010). Performance-Based Plastic Design of Earthquake Resistant Steel Structures: Concentrically Braced Frames, Tall Moment Frames, Plate Shear Wall Frames. *PhD Dissertation*, The University of Texas at Arlington.
- CSI (2007). Perform-3D v.4.0 User Manual. Computers & Structures Inc., Berkeley, CA.
- Federal Emergency Management Agency (FEMA). FEMA P695 (2009). Recommended Methodology for Quantification of Building System Performance and Response Parameters, Project ATC-63
- Goel, S.C., and Chao, S.H. (2008). Performance-Based Plastic Design: Earthquake-Resistant Steel Structures. International Code Council, USA.
- Gupta, A. and Krawinkler, H. (1999). Seismic Demands for Performance Evaluation Steel Moment Resisting Frame Structures. Report No. 132, The John A. Blume Earthquake Engineering Center, Dept. of Civil and Env Eng., Stanford University.
- Krawinkler, H (1978). Shear in Beam-Column Joints in Seismic Design of Steel Frames. *Engineering Journal, American Institute of Steel Construction*. Vol.5, No. 3: 82-91
- Pacific Earthquake Engineering Research Center (PEER). *PEER NGA database flatfile*. <http://peer.berkeley.edu/nga/flatfile.html> [10 September 2011]
- SAC Joint Venture for the Federal Emergency Management Agency (1994). Proceedings of the International Workshop on Steel Moment Frames. SAC 95-01.
- Somerville, P.G., Smith, M., Punyamurthula, S. and Sun, J. (1997). Development of Ground Motion Time Histories for Phase 2 of the FEMA/SAC Steel Project. Report No. SAC/BD-97/04, SAC Joint Venture, Sacramento, CA.
- UBC (1994). Uniform Building Code, International Conference of Building Officials, Whittier, California.
- Yang, T.Y., Moehle, J., Stojadinovic, B., and Der Kiureghian, A. (2009a). Seismic Performance Evaluation of Facilities: Methodology and Implementation. *Journal of Structural Engineering*, **135:10**, 1146–1154.
- Yang, T.Y., Moehle, J. & Stojadinovic, B. (2009b). Performance evaluation of innovative structural framing systems. *PEER report*, Pacific Earthquake Engineering Research Center, University of California, Berkeley. Report number 2009/103.